VIP Biochemical Networks Very Important Paper

DOI: 10.1002/anie.201402327

Threshold Sensing through a Synthetic Enzymatic Reaction–Diffusion Network**

*Sergey N. Semenov, Albert J. Markvoort, Tom F. A. de Greef, and Wilhelm T. S. Huck**

Dedicated to Professor George M. Whitesides on the occasion of his 75th birthday

Abstract: *A wet stamping method to precisely control concentrations of enzymes and inhibitors in place and time inside layered gels is reported. By combining enzymatic reactions such as autocatalysis and inhibition with spatial delivery of components through soft lithographic techniques, a biochemical reaction network capable of recognizing the spatial distribution of an enzyme was constructed. The experimental method can be used to assess fundamental principles of spatiotemporal order formation in chemical reaction networks.*

The remarkable ability of biological systems to respond and adapt to their environment is to a large extent regulated through complex enzymatic reaction networks such as signaling cascades.[1] The biochemical reactions lead to changes in the local concentrations of proteins, and slow diffusion results in a nonhomogeneous distribution of components.[2] In recent years, a picture has emerged that shows how living systems can control the spatiotemporal organization of their biochemical reaction networks by carefully tuning the reaction and diffusion of the molecular components.[3,4] A major challenge for chemistry is to master a similar level of control over chemical reaction networks in synthetic systems. Elegant examples of synthetic reaction–diffusion systems exist,[5] and recent progress has shown how functionality can be introduced. For example, programmable transformations of patterns and edge detection have been demonstrated with the Belousov–Zabotinsky reaction,[6] DNA-based reaction–diffusion networks,[7] or colonies of genetically engineered bacteria.[8] We aim to construct synthetic enzymatic reaction networks because enzymatic activities can be tuned with other enzymes or small molecules and can thus be used as computational elements.[1,4,9–11]

We investigated how enzymatic reaction networks can be used to "sense" the spatial distribution of enzymes and translate this information into a yes/no "signal". We recently described a simple biochemical model system that mimics the spatial propagation of enzymatic activity in a confined environment.[12] The controlled diffusion of proteins or enzymes from micropatterned agarose gels into hydrogels modified with ligands or fluorogenic substrates (Figure 1 a) is a convenient method to quantitatively study reaction–diffusion processes.[13] Previously, we studied the diffusion of trypsin into a gel containing both substrate and a strong competitive inhibitor. The latter resulted in nonlinear enzyme kinetics in the gel caused by the so-called molecular titration effect,[14] and this allowed us to control the spatial and temporal characteristics of the enzymatic diffusion front.

To sense the spatial distribution and filter noise, we inserted a filtering layer containing the strong competitive inhibitor soybean trypsin inhibitor (STI),[15] which influences the spatiotemporal evolution of enzymatic activity in a substrate-laden gel (Figure 1). A yes/no response was achieved through the introduction of a positive feedback loop through the autocatalytic activation of enzymatic activity inside a gel loaded with freely diffusing inhibitor and cross-linked substrate. The coupling of autocatalysis and molecular titration leads to a threshold of enzymatic activity (Figure 2). Finally, we combine ultrasensitivity and positive feedback loops with a filtering layer containing freely diffusible inhibitor to digitally decode the spatial density of input signals (Figure 3).

A schematic representation of our experimental methods is shown in Figure 1. In an extension of previous setups,[12] we introduce an additional polyacrylamide (PAAm) gel layer with covalently attached inhibitor between the micropatterned agarose stamp containing trypsin and the PAAm gel containing cross-linked fluorogenic substrate. When inhibitor is present in the intermediate layer, the free trypsin is buffered by molecular titration and free trypsin is only present after the inhibitor sink is filled.[12] As is observed from the kymographs displayed in Figure 1 b, buffering the free trypsin results in a strong dependence of the arrival time of the enzyme diffusion front as it enters the substrate layer on the width of the micropatterned pillars of the agarose stamp, while this correlation dramatically weakens in the absence of inhibitor. Quantitative analysis of the data by using a partial differential equation (PDE) model reveals excellent agree-

[*] Dr. S. N. Semenov, Prof. Dr. W. T. S. Huck
Department of Physical Organic Chemistry, Radboud University Nijmegen, Institute for Molecules and Materials
Heyendaalseweg 135, 6525 AJ Nijmegen (The Netherlands)
E-mail: w.huck@science.ru.nl
Homepage: http://www.ru.nl/physicalorganicchemistry/
Dr. A. J. Markvoort, Dr. T. F. A. de Greef
Computational Biology Group, Department of Biomedical Engineering and Institute for Complex Molecular Systems
Eindhoven University of Technology
Den Dolech 2, 5600 MB Eindhoven (The Netherlands)

[**] We acknowledge financial support from the European Research Council (ERC; Advanced Grant 246812 Intercom (W.T.S.H.)), the Netherlands Organisation for Scientific Research (NWO; VENI Grant: 722.012.001 (T.F.A.d.G.), VICI Grant 700.10.44 (W.T.S.H.) a Marie Curie Intra-European Fellowship (Grant 300519 (S.N.S.)) and funding from the Ministry of Education, Culture and Science (Gravity program 024.001.035). We acknowledge Dr. V. Chokkalingam for his help with photolithography.

Supporting information for this article is available on the WWW under http://dx.doi.org/10.1002/anie.201402327.

 © 2014 Wiley-VCH Verlag GmbH & Co. KGaA, Weinheim

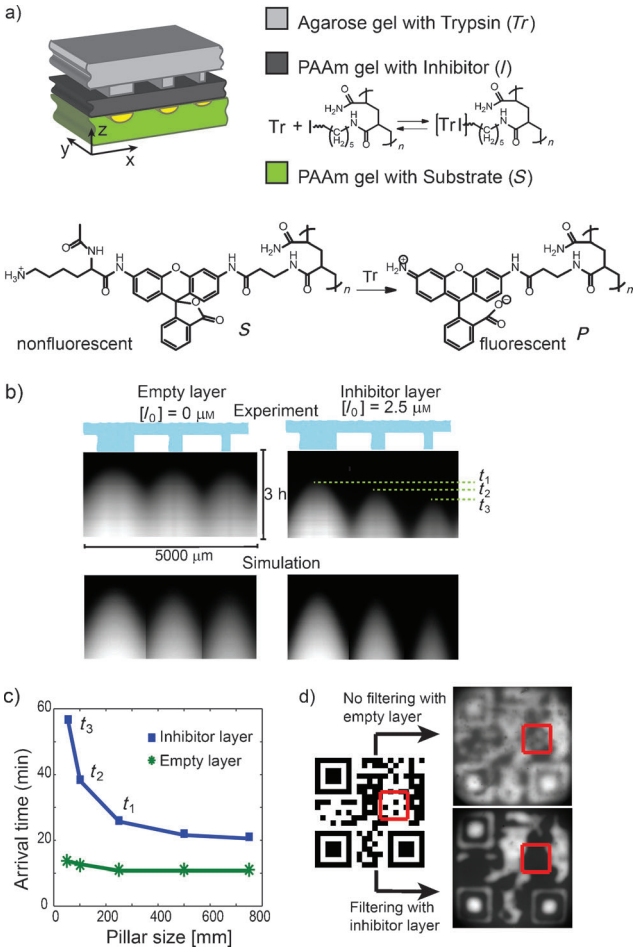

Figure 1. a) Schematic representation of a wet stamping experiment in which trypsin (*Tr*, 86 μM) diffuses from a spatially encoded stamp into a multilayered gel consisting of a thin gel layer (0.4 mm) containing nonfunctionalized (empty) or inhibitor (*I*, 2.5 μM) functionalized PAAm and a thicker gel layer (1 mm) containing PAAm cross-linked with fluorogenic substrate *S*, which is converted to fluorescent product *P*. The spatially modulated agarose stamp consists of microfabricated pillars of varying width (250, 100, 50 μm). b) Comparison of experimental (top) and theoretical (bottom) kymographs obtained by wet stamping of trypsin ($[Tr_0]=2$ mg mL^{-1}) from spatially modulated stamps onto multilayered gels consisting of an empty ($[I_0]=0$ μM) and substrate layer (left) or an inhibitor ($[I_0]=2.5$ μM) and substrate layer (right). The substrate concentration ($[S_0]$) is 0.1 mg mL^{-1} in both experiments. t_1-t_3 are the arrival times of the enzyme front. c) Calculated arrival time of the enzyme front in the substrate layer as a function of pillar width for both cases. The arrival time is defined as the time by which 1% of the substrate in the grid point closest to the center of a pillar, while still in the substrate layer, is converted into product. Simulated kymographs were obtained by using the following parameters: $D_e=1.8\times10^{-11}$ m^2 s^{-1}, $k_{cat}/K_d=4.7\times10^2$ s^{-1} M^{-1} and $K_i=10^{-9}$ M. d) Spatial filtering of small-scale features. The fluorescent micrographs were taken at $t=40$ min (empty layer) and $t=76$ min (inhibitor layer)

ment between the experimental and computed kymographs. In the presence of inhibitor, the computational analysis confirms the strong dependence of the arrival time on pillar width (Figure 1c) when the size of the pillars becomes smaller than the thickness of the intermediate layer. In this regime, diffusion of the enzyme from the agarose stamp can be approximated as a point source and the diffusion front of the enzyme in the intermediate layer has a strong radial character. When this is the case, buffering of the free enzyme by the inhibitor has a strong effect on the propagation speed of the front (see the Supporting Information). By contrast, when the pillar width is larger than the thickness of the intermediate layer, the enzyme diffusion front in the intermediate layer becomes effectively one-dimensional and further increasing the pillar size does not influence the front propagation speed. To illustrate how this relationship can be used to modulate the spatial patterns of the input, we designed a stamp with a 2D barcode containing both large and small squares. Only signals from larger features are visible in the substrate layer while smaller features are filtered out as a result of slow propagation of the enzyme front through the intermediate inhibitor layer (Figure 1d and the Supporting Information for full details).

From these experiments we can conclude that the inhibitor in the intermediate layer functions as an analog modulator and converts an input signal, proportional to the feature size on the agarose stamp, into an output signal consisting of varying arrival times of the enzyme front in the substrate layer. Previous computational work has shown that biochemical reaction–diffusion networks can be constructed to function as analog-to-digital converters.[16] In our system, a digital response is engineered by combining molecular titration (ultrasensitivity) with positive feedback (amplification) in the gel containing the fluorogenic substrate. Positive feedback is introduced through an enzyme that catalyzes its own formation. For this we employ the well-known autocatalytic formation of trypsin from trypsinogen (*Tg*).[17] By loading the gel containing cross-linked substrate with freely diffusible *Tg* and inhibitor and ensuring that self-activation of *Tg* is minimal, free trypsin diffusing from the stamp may initiate a traveling autocatalytic wave of enzymatic activity (Figure 2).

In this experiment, the input signal is a combination of 1) concentration of trypsin in the stamp, 2) pillar width, and 3) the period of time for which the stamp is in conformal contact with the gel. The output signal is again the fluorescence intensity arising from converted product, which indicates whether or not a traveling autocatalytic wave of enzymatic activity is initiated from a pillar. We fixed the trypsin concentration in the stamp at 2 mg mL^{-1}, used stamps with three different pillar widths (50, 100, and 250 μm), and varied the contact time until activation was observed. The kymographs of experiments employing a 2 min contact time are shown in Figure 2b. Three distinct zones can be observed: i) trypsin from the stamp spreads into the gel, ii) trypsinogen activation competes with trypsin inactivation as the diffusion front of trypsin encounters the freely diffusible inhibitor, and iii) autocatalytic activation of trypsin from trypsinogen leads to a traveling wave. The middle zone is crucial for propagation of the trypsin diffusion front. In this zone, there is a critical balance between initial diffusion of trypsin from the stamp, second-order autocatalytic production of trypsin from trypsinogen, and diffusion of inhibitor from other regions in the gel, which results in the formation of an inactive enzyme–inhibitor complex. Because the autocatalytic production of trypsin from trypsinogen is second-order, the total production

 © 2014 Wiley-VCH Verlag GmbH & Co. KGaA, Weinheim

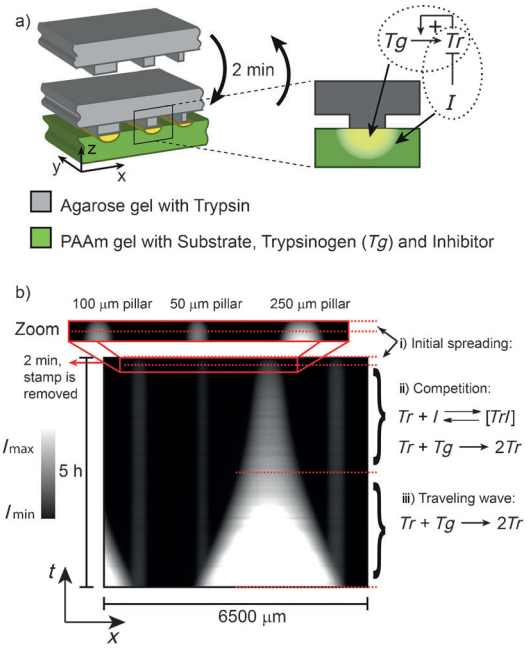

Figure 2. a) Schematic representation of a wet stamping experiment in which trypsin (86 μM) diffuses for 2 min from a spatially encoded stamp into a PAAm gel layer (1 mm) containing trypsinogen (86 μM), freely diffusible inhibitor (2.5 μM), and cross-linked fluorogenic substrate (0.1 mg mL^{-1}). The spatially modulated agarose stamp consists of microfabricated pillars of varying width (250, 100, 50 μm). The insert illustrates how autocatalysis prevails in the center of the diffusion zone, whereas inhibition competes at the diffusion front. b) Kymograph and schematic illustration of reactions occurring in different zones.

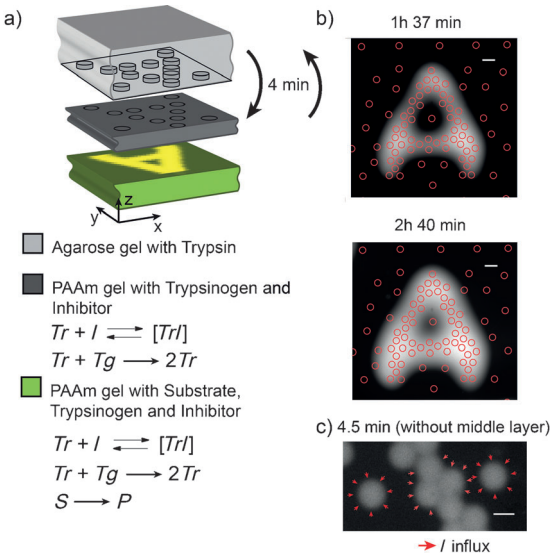

Figure 3. Recognition of pillar density by the chemical reaction network. a) Scheme of the experiment and contents of the layers. Inhibitor is freely diffusible. Concentrations: [*Tr*] = 86 μM, [*Tg*] = 86 μM, [*I*] = 2.5 μM) and [*S*) = 0.1 mg mL^{-1}. b) Fluorescence images of the bottom layer. Red circles illustrate the position of the pillars in the activator stamp. Scale bars: 300 μm. c) Omission of the middle layer leads to activation under each pillar. The red arrows show how isolated pillars are completely surrounded by diffusive influx of inhibitor, in contrast to clustered pillars. Scale bar: 150 μm.

rate of trypsin in a region below the stamp is proportional to the total amount of free trypsin (see the Supporting Information). If the influx of freely diffusing inhibitor from other regions in the gel surpasses the autocatalytic production, all newly produced trypsin becomes immediately inactivated through binding to the inhibitor and front-propagation failure occurs. However, if the production rate is higher than the influx of inhibitor, the amount of free trypsin, and consequently the autocatalytic production, increases exponentially. Trypsin then spreads autocatalytically through the gel, thereby resulting in a traveling wave moving at near-constant speed, as is also observed in the case for the pH waves induced in glucose oxidase[18] and urease[19] catalyzed reactions. If initial diffusion of trypsin originates from a small contact area, the diffusion profile will have a strong radial component characterized by a high surface to volume ratio. As a result, the total influx of inhibitor is sufficient to inactivate all trypsin and propagation failure occurs. However, for larger contact areas, the diffusion profile will be one-dimensional and the lower surface to volume ratio results in a relatively smaller inhibitor influx. Indeed, we observe front propagation for larger pillars (250 μm) but not for smaller pillars.

In the final part of this work, we demonstrate how the density of features can determine whether an autocatalytic wave is triggered in the bottom gel. In contrast to the variation in signal intensity shown in Figure 2, where different widths of lines were used, we now produce a micropattern consisting of numerous 150 μm spots distributed nonrandomly on the stamp (Figure 3). The micropatterned agarose stamp is placed on an intermediate layer for approximately 4 min. This layer contains freely diffusible inhibitor and *Tg*. As trypsin diffuses through the "filter" layer, the diffusion profile of spots that are in close proximity will start to overlap. Consequently, the contact area between the trypsin and inhibitor front is smaller and the influx of inhibitor per unit of trypsin is less for dense pillars than for isolated ones (Figure 3c). As a result, the influx of trypsin from the stamp to the intermediate layer will locally trigger the autocatalytic wave shown in Figure 2 only in dense areas. This autocatalytic wave then reaches through to the bottom readout layer and a fluorescence signal is observed only where spots are sufficiently close (Figure 3b).

In conclusion, we have shown how fairly complex properties can emerge in a relatively simple system consisting of gels with an enzyme and its pro-enzyme, a strong inhibitor, and a fluorogenic substrate. These properties are not present in the individual components but are "systems properties" and they arise from the connectivity of the enzymatic reactions and the coupling between reactions and the diffusion of components. Key to the design of the reaction–diffusion network is the combination of an autocatalytic reaction with ultrasensitivity generated by molecular titration. Herein, we have shown a network that can filter out certain aspects of a pattern (by density of pillars or size of features on a stamp) and translate this information into a fluorescent signal through the local autocatalytic activation of trypsin. This example is just one of the properties that can

 © 2014 Wiley-VCH Verlag GmbH & Co. KGaA, Weinheim

be encoded in such systems, and we envisage that future generations of "smart materials" will incorporate more complex versions of enzymatic reaction–diffusion networks.[20] Such materials might be able to sense, to learn, to adapt, and to make autonomous decisions, as stated so eloquently in a recent paper by Jean-Marie Lehn.[21]

Experimental Section

Synthesis of substrate functionalized polyacrylamide (PAAm) hydrogels. Substrate functionalized PAAm hydrogels were prepared according to literature procedures. Prepolymer solution containing acrylamide (9.7%), bis-acrylamide (0.4%), and required amounts of acrylamide-functionalized fluorogenic substrate (*S*) was casted between two hydrophobic glass slides separated by a thin spacer (1.0 or 0.4 mm). The *N*-acryloyl-ε-aminohexanoic acid modified STI was added to the prepolymer solution to obtain STI-modified gels. Polymerization was initiated with ammonium persulfate (APS) and tetramethylethylendiamine (TEMED). Hydrogels were stored in 10 mM Tris buffer (pH 7.8). Agarose stamps were prepared by casting hot agarose solution against PDMS master.

WET stamping, data Collection and data Treatment. The modified wet stamping procedure reported by Grzybowski et al.[13b] was used. A functionalized PAAm gel (1 × 1.5 cm) was soaked in buffer (10 mM Tris pH 7.8, 20 mM $CaCl_2$) containing appropriate amounts of the inhibitor and trypsinogen and equilibrated in solution for at least 12 hr. A 6% agarose stamp was soaked in a solution of trypsin in buffer (10 mM Tris pH 7.8, 20 mM $CaCl_2$) for at least 20 h at 4 °C. The piece of PAAm gel was then placed on a glass slide and dried for 30 seconds (care was taken to prevent the formation of air bubbles between the glass slide and the gel.) The agarose stamp was brought into contact (feature-side down) with the PAAm gel. The obtained construct was covered by a plastic cup containing a piece of wet cotton to prevent drying during an experiment and was placed on the microscope stage. The contact of the stamp pillars with the PAAm gel was brought in focus and a series of fluorescence images were acquired. All experiments were performed on an inverted epifluorescence microscope (IX81, Olympus) equipped with a high pressure mercury lamp (Olympus), U-FGFP filter cube (Olympus), iXon 897 camera (Andor), and a 2 × (Plan, 0.06 NA, Olympus) objective.

Received: February 12, 2014
Published online: April 2, 2014

Keywords: biochemical networks · biosensors · enzyme catalysis · reaction–diffusion systems · ultrasensitivity

[1] M. Behar, A. Hoffmann, *Curr. Opin. Genet. Dev.* **2010**, *20*, 684 – 693.
[2] a) S. Soh, M. Byrska, K. Kandere-Grzybowska, B. A. Grzybowski, *Angew. Chem.* **2010**, *122*, 4264 – 4294; *Angew. Chem. Int. Ed.* **2010**, *49*, 4170 – 4198; b) E. Karsenti, *Nat. Rev. Mol. Cell Biol.* **2008**, *9*, 255 – 262; c) A. Kicheva, M. Cohen, J. Briscoe, *Science* **2012**, *338*, 210 – 212; d) A. D. Lander, *Cell* **2011**, *144*, 955 – 969.
[3] J. Wagner, J. Keizer, *Biophys. J.* **1994**, *67*, 447 – 456.
[4] O. Brandman, T. Meyer, *Science* **2008**, *322*, 390 – 395.
[5] A. Padirac, T. Fujii, A. Estevez-Torres, Y. Rondelez, *J. Am. Chem. Soc.* **2013**, *135*, 14586 – 14592; b) X. L. Liao, R. T. Petty, M. Mrksich, *Angew. Chem.* **2011**, *123*, 732 – 734; *Angew. Chem. Int. Ed.* **2011**, *50*, 706 – 708.
[6] L. Kuhnert, K. I. Agladze, V. I. Krinsky, *Nature* **1989**, *337*, 244 – 247.
[7] S. M. Chirieleison, P. B. Allen, Z. B. Simpson, A. D. Ellington, X. Chen, *Nat. Chem.* **2013**, *5*, 1000 – 1005.
[8] J. J. Tabor, H. M. Salis, Z. B. Simpson, A. A. Chevalier, A. Levskaya, E. M. Marcotte, C. A. Voigt, A. D. Ellington, *Cell* **2009**, *137*, 1272 – 1281.
[9] a) A. Boiteux, A. Goldbeter, B. Hess, *Proc. Natl. Acad. Sci. USA* **1975**, *72*, 3829 – 3833; b) E. Fung, W. W. Wong, J. K. Suen, T. Bulter, S. G. Lee, J. C. Liao, *Nature* **2005**, *435*, 118 – 122.
[10] a) D. Bray, *Nature* **1995**, *376*, 307 – 312; b) G. Strack, M. Ornatska, M. Pita, E. Katz, *J. Am. Chem. Soc.* **2008**, *130*, 4234 – 4235.
[11] a) N. E. Buchler, M. Louis, *J. Mol. Biol.* **2008**, *384*, 1106 – 1119; b) A. Goldbeter, D. E. Koshland, *Proc. Natl. Acad. Sci. USA* **1981**, *78*, 6840 – 6844.
[12] S. N. Semenov, A. J. Markvoort, W. B. L. Gevers, A. Piruska, T. F. A. de Greef, W. T. S. Huck, *Biophys. J.* **2013**, *105*, 1057 – 1066.
[13] a) B. A. Grzybowski, Y. H. Wei, P. J. Wesson, I. Kourkine, *Anal. Chem.* **2010**, *82*, 8780 – 8784; b) C. J. Campbell, R. Klajn, M. Fialkowski, B. A. Grzybowski, *Langmuir* **2005**, *21*, 418 – 423.
[14] J. E. Ferrell, Jr., *Trends Biochem. Sci.* **1996**, *21*, 460 – 466.
[15] A. Luthy, M. Praissman, W. R. Finkenstadt, M. Laskowski, *J. Biol. Chem.* **1973**, *248*, 1760 – 1771.
[16] A. Lipshtat, G. Jayaraman, J. C. He, R. Iyengar, *Proc. Natl. Acad. Sci. USA* **2010**, *107*, 1247 – 1252.
[17] H. Neurath, W. J. Dreyer, *Discuss. Faraday Soc.* **1955**, *20*, 32 – 43.
[18] D. G. Miguez, V. K. Vanag, I. R. Epstein, *Proc. Natl. Acad. Sci. USA* **2007**, *104*, 6992 – 6997.
[19] M. M. Wrobel, T. Bansagi, S. K. Scott, A. F. Taylor, C. O. Bounds, A. Carranzo, J. A. Pojman, *Biophys. J.* **2012**, *103*, 610 – 615.
[20] X. M. He, M. Aizenberg, O. Kuksenok, L. D. Zarzar, A. Shastri, A. C. Balazs, J. Aizenberg, *Nature* **2012**, *487*, 214 – 218.
[21] J.-M. Lehn, *Angew. Chem.* **2013**, *125*, 2906 – 2921; *Angew. Chem. Int. Ed.* **2013**, *52*, 2836 – 2850.

 © 2014 Wiley-VCH Verlag GmbH & Co. KGaA, Weinheim